Proc. Natl. Acad. Sci. USA
Vol. 90, pp. 11648–11652, December 1993
Biochemistry

Val → Ala mutations selectively alter helix–helix packing in the transmembrane segment of phage M13 coat protein

CHARLES M. DEBER*†‡, AMIR R. KHAN*†, ZUOMEI LI*†, CAROLIN JOENSSON*†, MIRA GLIBOWICKA*†, AND JING WANG§

*Division of Biochemistry Research, Research Institute, Hospital for Sick Children, Toronto, ON, Canada M5G 1X8; and †Department of Biochemistry and §Medical Research Council Group in Membrane Biology, Department of Medicine, University of Toronto, Toronto, ON, Canada M5S 1A8

Communicated by Elkan Blout, September 16, 1993

ABSTRACT **Val → Ala mutations within the effective transmembrane segment of a model single-spanning membrane protein, the 50-residue major coat (gene VIII) protein of bacteriophage M13, are shown to have sequence-dependent impacts on stabilization of membrane-embedded helical dimeric structures. Randomized mutagenesis performed on the coat protein hydrophobic segment 21–39 (YIGYAWAMVVVIVGATIGI) produced a library of viable mutants which included those in which each of the four valine residues was replaced by an alanine residue. Significant variations found among these Val → Ala mutants in the relative populations and thermal stabilities of monomeric and dimeric helical species observed on SDS/PAGE, and in the range of their α-helix → β-sheet transition temperatures confirmed that intramembranous valine residues are not simply universal contributors to membrane anchoring. Additional analyses of (*i*) nonmutatable sites in the mutant protein library, (*ii*) the properties of the double mutant V29A-V31A obtained by recycling mutant V31A DNA through mutagenesis procedures, and (*iii*) energy-minimized helical dimer structures of wild-type and mutant V31A transmembrane regions indicated that the transmembrane hydrophobic core helix of the M13 coat protein can be partitioned into alternating pairs of potential protein-interactive residues (V30, V31; G34, A35; G38, I39) and membrane-interactive residues (M28, V29; I32, V33; T36, I37). The overall results constitute an experimental approach to categorizing the distinctive contributions to structure of the residues comprising a protein–protein packing interface vs. those facing lipid and confirm the sequence-dependent capacity of specific residues within the transmembrane domain to modulate protein–protein interactions which underlie regulatory events in membrane proteins.**

Although most transmembrane (TM) regions of integral membrane proteins are presumed to be α-helical in conformation, glycine and β-branched residues (valine, isoleucine, threonine), known to disfavor α-helices in soluble proteins (1), often account for nearly 50% of TM amino acids (2). As many membrane proteins require function-related conformational change(s) [e.g., during membrane insertion (3) or signaling (4)], the TM sequence—particularly through its glycine and β-branched content—may also contribute to function (e.g., conformational flexibility and/or helix destabilization) at various stages of the protein life cycle (5) rather than serve exclusively to anchor the protein to the membrane.

The prevalence of β-branching in TM segments is epitomized by the major coat (gene VIII) protein of bacteriophage M13, of which the mature 50-residue sequence after excision of its signal sequence by *Escherichia coli* leader peptidase is AEGDDPAKAAFNSLQASATEYIGYAWAMVVVIVGATIGIKLFKKFTSKAS [ref. 6; a stretch of 19 uncharged residues (the candidate TM region), 21–39, is underlined]. M13 coat protein experiences a variety of environments during the phage life cycle, from its initial DNA-bound state and its deposition in the host inner membrane, to its presence in the host cytoplasm during biosynthesis and membrane insertion. In the viral assembly/extrusion stage, old as well as newly synthesized coat protein participates in an α-helical aggregation process within the membrane, ultimately encapsulating viral DNA (7, 8). In contrast, the transient existence of coat protein in the *E. coli* cytosol must favor a water-soluble conformation, in which nascent membrane proteins are likely to have a β-sheet ("extended") conformation (9). The sequences of a variety of filamentous phage coat proteins tend to be highly conserved, perhaps reflecting an inherent requirement for multiple conformations dictated by primary sequence during the phage life cycle (10).

DNA-bound M13 coat proteins are essentially 100% α-helical, while helical aggregates are believed to be intermediate states in the host inner membrane during phage assembly (11). Considered a model single-spanning membrane protein, wild-type (WT) coat protein has been deduced to exist largely as a helical dimer in 2.5 mM SDS micelles and in 30 mM deoxycholate (12). The conformation of the related Pf1 phage coat protein in a micelle environment is proposed to consist of two α-helical regions along its full sequence—an aqueously located N-terminal helix and a TM plus C-terminal helix—with the two segments linked by a short region of more flexible structure (13).

Previous work in this laboratory (5, 14, 15) has focused on the site-directed mutagenesis of the TM region of M13 coat protein, with a primary goal of identifying TM residues which contribute specifically to coat protein structure and function. An initial library of 28 viable mutants generated in the putative TM region demonstrated that coat protein can accommodate significant changes in side-chain chemistry, volume, and charge (15). The methodology allows for production of mutant coat proteins in milligram quantities and is accordingly amenable to circular dichroism (CD) and nuclear magnetic resonance spectroscopy (NMR) studies (5, 14). In the present work, we take advantage of a subset of mutants in which each of the M13 TM region valine residues is replaced with alanine (V29A, V30A, V31A, and V33A). These mutants afford an opportunity to "walk" alanine residues through the valine-rich core segment and thereby to explore the sequence-dependent structural role(s) of valines within TM helices. Through biophysical analyses of these latter mutants, and of a double mutant (V29A-V31A) obtained by subjecting the valine-rich TM region of M13 coat protein to a further cycle of mutagenesis, we demonstrate the TM position dependence of Val-mediated protein–protein and protein–lipid interactions.

The publication costs of this article were defrayed in part by page charge payment. This article must therefore be hereby marked "*advertisement*" in accordance with 18 U.S.C. §1734 solely to indicate this fact.

Abbreviations: TM, transmembrane; WT, wild type.

‡To whom reprint requests should be sent at the * address.

MATERIALS AND METHODS

Mutagenesis of M13 Coat Protein. Mutagenesis was performed with an oligonucleotide-directed mutagenesis kit, (Amersham) based on the method of Eckstein and coworkers (16). In addition to WT M13mp18 single-stranded DNA (Pharmacia), three mutant single-stranded DNAs, each with a single Val → Ala mutation in the coat protein TM region (V29A, V30A, and V31A), were used as mutagenesis templates. (Mutant V33A exhibited poorer growth characteristics and was reserved for future investigation.) Three overlapping oligonucleotides, which together spanned the entire TM region, residues 21–39), were used to anneal directly to the template (15); no subcloning was required. Oligonucleotides were synthesized at the Biotechnology Centre, Banting Institute, University of Toronto, and purified with oligonucleotide-purification cartridges (Applied Biosystems). To assess the tolerance of M13 phage to TM mutations, "randomized" oligonucleotides were used which contained 92.5% WT precursor at each selected site but also 2.5% "contaminants" of each of the other three nucleotides (17). In each oligonucleotide, the 3′-end base was not randomized. Nine separate mutagenesis reactions (3 templates × 3 oligonucleotides) were performed. Oligonucleotide sequences were: 5′-CGCCCACGCATAACCGATATAT-3′ (V29A, V30A, V31A oligonucleotide 1; coat protein residues 21–27); 5′-GACAATGACAACAGCCATCGCC-3′ (V29A oligonucleotide 2; residues 27–33); 5′-GACAATGACAGCAACCATCGCC-3′ (V30A oligonucleotide 2; residues 27–33); 5′-GACAATGGCAACAACCATCGCC-3′ (V31A oligonucleotide 2; residues 27–33); 5′-GATACCGATAGTTGCGCCGACA-3′ (V29A, V30A, V31A oligonucleotide 3; residues 33–39). After mutagenesis, 440 plaques were sequenced (195 for oligonucleotide 1, 120 for oligonucleotide 2, and 125 for oligonucleotide 3). A total of 48 mutations (including silent) were identified, for an overall efficiency of 11%.

Preparative-Scale Samples of Mutant M13 Proteins. Mutant phages were amplified by infecting 1-liter cultures of *E. coli* JM101 (15). Coat protein mutants were separated from DNA by gel filtration [Sephacryl S-200 HR column (Pharmacia) equilibrated with 8 mM sodium deoxycholate/25 mM sodium borate elution buffer] (18).

CD Spectra. CD spectra were recorded on a Jasco J-720 spectropolarimeter, with coat protein at 1 mg/ml in 30 mM deoxycholate/25 mM sodium borate, pH 9. Coat protein concentrations were determined by A_{280} with an extinction coefficient of 1.66 for 1 mg/ml (15). Each curve was the average of four to six scans, recorded at 250 to 190 nm in a cell (Jasco) with a path length of 0.1 mm.

Molecular Modeling. Model building and energy minimization were performed with the CHARMM22 program (19) using full-atom representation and empirical energy functions. The conjugated gradient Powell method and adopted basis Newton–Raphson method were used for the minimization task. The conformation of a 19-residue TM helix of M13 coat protein (residues 24–42) was built (see also refs. 20 and 21), with acetylated N terminus and methyl-amidated C terminus. Standard bond lengths and bond angles were used, with α-helical (ϕ, ψ, ω) and extended (antiperiplanar) side-chain χ angles. The dielectric constant was set at 1 to mimic the nonpolar environment of the lipid bilayer. After optimization of the monomer helix, a dimer was constructed by duplication, rotation, and translation of the monomer. With helix 1 fixed in space, helix 2 was rotated around its z axis by increments of 10° and minimized at each rotation angle. The tilt of helix 2 relative to helix 1 was varied from −60° to 60° for each rotation angle and minimization was repeated. Helix 1 was rotated around its axis by increments of 30° and the minimization procedure described for helix 2 was repeated. For each dimer conformation, the total energy was minimized with full degrees of freedom of the system. The lowest minimum-energy structures thus obtained were subjected to room temperature (300 K) molecular dynamics simulations (4-ps heating, 12-ps equilibration, and 12-ps production) (19). The residue–residue interaction energies were calculated at each 50-fs interval during the simulated molecular dynamics trajectory in the final productive stage. The average values of these energies were taken as a measurement of interaction between residues.

RESULTS

Viable Multiple-Site Mutations of M13 Coat Protein TM Region. Upon cycling of single-stranded DNAs of coat protein single mutants V29A, V30A, and V31A through the randomized mutagenesis procedure, 33 new single-, double- and triple-site amino acid substitutions were generated, bringing the total number of viable M13 TM-region mutants to 61 (Table 1). This procedure provided the mutant V29A-V31A, whose properties are further investigated herein. Overall, 35 of 61 mutants feature decreased β-branching, strongly reinforcing the observation that WT β-branched amino acid content must already be near-maximal for function (14). While glycine was statistically highly probable at eight sites (residues 25–27, 29–31, 33, and 35 can each mutate to glycine by a single nucleotide change), none of the 61 mutants had increased glycine content, suggesting a critical packing role for glycine within the membrane (see below). Of the 27 Val → Ala background mutants, 21 were compatible with phage viability irrespective of whether the background was valine (WT) or alanine (G23A, G23A-V29A, Y24H, Y24H-V30A, etc.). Thus, rather than revertants (i.e., Ala → Val mutations compensating for the V29A, V30A, or V31A loss in β-branching or net hydrophobicity), mutations obtained by recycling were essentially independent of the alanine background. These results provide evidence that although the mutagenic oligonucleotides are random, the library remains a function of viability.

The tolerance of the M13 coat protein TM region to mutation is apparent from mutants such as V29A-V31L-I32T, which features three changes within a span of four residues; G23R-V29A, which places a positive charge at the N terminus of the TM helix, and Y24C-V31A, which introduces the

Table 1. Viable-mutant library of the putative TM segment of M13 coat protein, as generated by application of the Eckstein method using randomized oligonucleotides to WT phage and to mutant phage DNAs of V29A, V30A, and V31A

I22V	Y24H	V29A-V31A
G23A	Y24H-A27E	V29A-V31L
G23A-V29A	Y24H-V29A	V29A-V31L-I32T
G23A-V31A	Y24H-V30A	V29I-V31T
G23D	Y24H-A27E-V30A	V29T
G23D-V29A	Y24N	V30A
G23D-V30A	Y24N-V31A	V30I
G23D-Y24A-V30A	Y24S-V31A	V31A
G23R-V29A	A25S-V31A	V31A-T36A
G23S	A27E	V31A-I37V
G23S-A25S	A27E-V30A	V31I
G23S-V30A	A27E-V31A	V31L
G23S-V31A	A27S	V31T
G23S-A27S-V29A	A27T	I32V
G23T-V30A	A27T-V30A	I32T
G23V-A27S	A27T-V31A	V33A
G23V-V31T	M28L	T36S
Y24A	M28L-V31A	I37V
Y24C-V31A	M28L-V31L	I37T
Y24D	V29A	G38S
Y24D-V29A		

potential for covalent disulfide-bonded dimers. Yet all single- or double-site mutations (with Val → Ala backgrounds) found in the TM core (residues 28–39) were uncharged (Fig. 1) and relatively conserved in hydrophobicity vs. WT protein. Many of these mutations correspond to residues which comprise the WT sequence of related filamentous bacteriophages [M28L, V31L, I32V, I37V for If1; V31T, I32V for IKe (22)]. Mutants involving Val → Thr changes (V29T, V31T, G23V-V31T, V29I-V31T) arise from stepwise two-base changes vs. WT codons, since oligonucleotides with (mutant) alanine codons can mutagenize to threonine codons with one base change.

SDS/PAGE to Probe the Thermostability of TM Mutant α-Helicity. Thermally induced *in vitro* α-helix → β-sheet transitions of WT M13 coat protein were noted by Spruijt *et al.* (11). In M13 coat protein TM mutants, these transitions were proposed to involve at least a two-step process (14), in which dissociation of intramembranous helical dimers/oligomers to monomers is followed by escape from the membrane and ultimately by water-based reassociation of the monomers into high molecular weight β-sheets. SDS/PAGE can therefore be used to assess relative populations and thermal stabilities of M13 coat protein species as a function of mutation type and locus (14). At 25°C, WT coat protein migrates in gels as a diffuse mixture of α-helical monomeric and dimeric species (Fig. 2); after brief heating at 95°C (5 min), these species are replaced by high molecular weight aggregates. Mutant V29A behaves similarly to WT coat protein; in addition, higher [probably helical (8, 11, 14)] oligomeric states may also be discerned in V29A gels. In contrast, mutants V29A, V31A, and V29A-V31A migrate almost exclusively as dimers, with the majority of protein remaining as dimers at 95°C. Mutant V30A behaved similarly to V31A in parallel experiments, whereas V33A behaved similarly to WT protein (data not shown).

Conformational Studies of Mutant Coat Proteins by CD Spectroscopy. CD spectroscopy was used to assess species conformations and to detect conformational interconversions. With samples similar to those used for SDS/PAGE, CD spectra recorded in deoxycholate micelles at 25°C for WT, V29A, V31A, and V29A-V31A showed largely helical conformations for each protein (Fig. 3). Spectra recorded immediately at 85°C revealed the residue-dependent extent of (irreversible) conversion to β-sheet aggregates: WT and V29A displayed largely β-type CD spectra, whereas V31A and V29A-V31A spectra remained α-helical, with only minor fraying of helicity.

In parallel CD experiments performed using stepwise heating (5°C increments, 5 min at each temperature), we measured the effective midpoint of the irreversible $\alpha \rightarrow \beta$ transition temperatures (T_{mid})—defined as the halfway point between the initial $[\theta]_{208}$ and a final value at which increasing temperature induced no further change—for WT coat and the various V → A mutants. The values obtained—V33A (75°C), WT (76°C), V29A (86°C), V30A (90°C), V31A (>93°C), and V29A-V31A (>93°C)—indicated that a decrease in valine tended to maintain (dimeric) α-helical structures in the micelle relative to WT, but with the range in T_{mid} suggesting varying contributions at each locus.

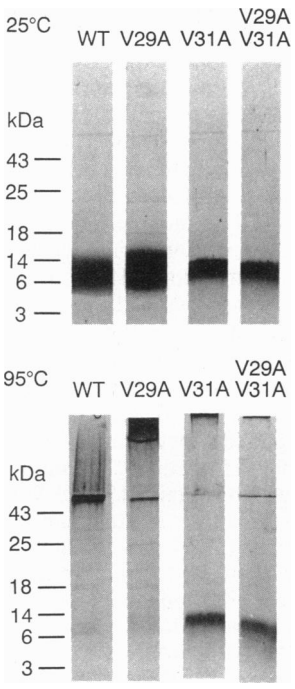

FIG. 2. SDS/PAGE analysis of WT and mutant coat proteins. Protein (4–5 μg) was loaded in a volume of 10 μl. Gels were run in 0.025 M Tris/0.192 M glycine/0.1% SDS, pH 8.3. Protein samples (1 mg/ml) were untreated (25°C) (*Upper*) or heated at 95°C for 5 min (*Lower*). Polymeric β-type aggregates, most apparent for WT and V29A, are seen both in the 5% stacking gel and at the interface between the stacking gel and the 15% separating gel.

Energy-Minimized Helical Dimers. The roles of individual valine residues in helix–helix packing were explored further with energy minimization/molecular dynamics simulation techniques. By using a 19-residue monomeric segment consisting of amino acids 24–42, which corresponds to a "shifted" TM span (residues 21–23 were excluded since results from the mutagenesis suggested the aqueous-accessible nature of this segment), dimers were constructed with each monomer in the α-helical conformation, from which a collection of energy minima was obtained for various helix–helix contact interfaces. Resulting energy-minimized molecular dynamics average structures for WT dimer and mutant V31A dimer are shown in helical ribbon representations in Fig. 4*a*. Space-filling models generated from these (Fig. 4*b*) indicate the favorable protein–protein interior packing of the combined four Val^{30} and Val^{31} residues of WT dimer; in the V31A dimer, both Val^{30} and the (now) mutant Ala^{31} residues remain located in this packing face. In contrast, Val^{29} and Val^{33} largely face lipid in both structures. Further analysis of the structures obtained confirmed the interior positions of Gly^{34}, Ala^{35}, and Gly^{38} in both proteins (data not shown). Analysis of residue–residue interaction energy suggests that the V31A mutation improves the intermolecular interaction energy at the mutation site and confers a general improvement of the interactions throughout the helix–helix interface. In particular, the interaction energies of the Ala^{27} residues with the opposing helices are clearly strengthened in the V31A mutant vs. WT dimer (data not shown), corresponding to a slight shift of the local helix–helix contact site from Trp^{26} to Ala^{27}; the improvement is also observed for Ala^{35} and Gly^{38}. Therefore, as may be discerned in Fig. 4*a*, the alanine-promoted packing

							arg	*cys*																										
							thr	*ser*																										
							val	Asp										Leu																
							Asp	Asn					Glu		*ile*			Thr															
							Ser	His					Thr		Thr	Ile		Ile	Thr					*ala*	Thr								
					Val		Ala	Ala	*ser*				Ser	Leu	Ala	Ala		Ala	Val		Ala			Ser	Val		Ser						
					|		|	|				|	|	|		|	|		|			|	|		|					
-Ala	Thr	Glu	Tyr		Ile		Gly	Tyr	Ala	Trp		Ala	Met	Val	Val		Val	Ile		Val	Gly	Ala	Thr	Ile		Gly	Ile	Lys	Leu	Phe-			
			21		22		23	24	25	26		27	28	29	30		31	32		33	34	35	36	37		38	39						

FIG. 1. Viable mutations arising along the 19-residue uncharged effective TM segment (Tyr^{21}–Ile^{39}) of M13 coat protein. The diagram was obtained from composite analysis of 61 mutants (Table 1). Single-site mutants are displayed above the WT TM sequence. Substitutions obtained only in double- or triple-site mutants are shown in italics and lowercase. Residues flanking the TM segment are indicated.

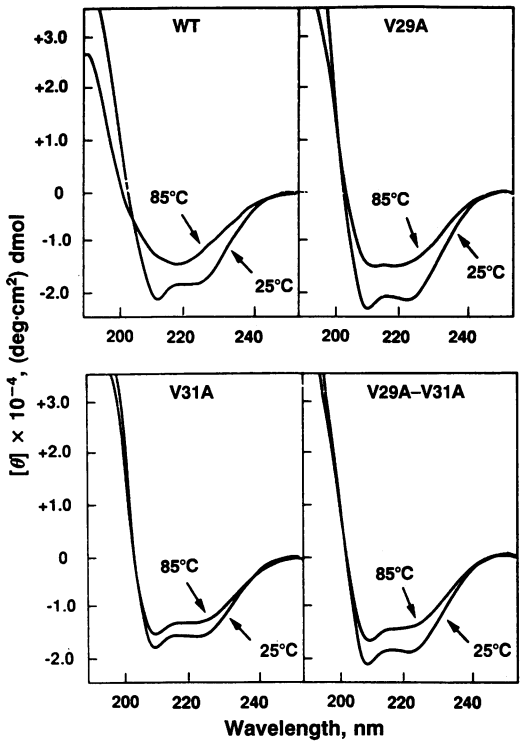

FIG. 3. CD spectra of WT M13 coat protein and mutants V29A, V31A, and V29A-V31A at 25°C and 85°C. Protein samples were 1 mg/ml in 30 mM deoxycholate/25 mM sodium borate, pH 9. Spectra were recorded at 25°C, after which the temperature was raised in 5°C increments, held at each temperature for 5 min, up to 85°C.

efficiency in mutant V31A propagates in both directions toward the termini of the TM segment.

Preliminary results from energy minimization of the V29A dimer (not shown) suggest, however, that the most stable arrangement for this mutant represents net rotations about the major axis of each protein chain (vs. WT and V31A), such that Ala^{29} becomes contained in the protein–protein packing face (while Val^{31} now faces lipid) to produce a dimer of lower energy than WT. This result accounts for the enhanced T_{mid} for V29A vs. WT. However, since at least one alanine (instead of valine) *must* face lipid in the V29A-V31A double mutant, the result that the V29A-V31A T_{mid} paralleled that observed for V31A is then explicable in terms of packing-driven helical dimer stability, rather than a net decrease in protein–lipid interactions by the "forced" interaction of Ala^{29} with lipid.

DISCUSSION

By recycling V29A, V30A, and V31A mutant M13 phage DNAs through Eckstein-based randomized mutagenesis protocols—allowing the coat protein to select for its own viability—we found the putative TM domain of M13 coat protein to be highly tolerant to second- and third-site mutations. Whatever conformational and protein–protein interactive properties are imparted by the WT segment 23–27 appeared to be essentially independent of any packing and/or hydrophobicity-mediated interactions in the lipid-interactive core (residues 28–39); i.e., the mutation spectrum at Gly^{23}, Tyr^{24}, and Ala^{27} was not modulated by the "background" Val → Ala mutations. Similarly, multiple-site mutations of λ repressor protein appeared to be mutually independent (23). Since polar-mutation-sensitive regions (in this case, Gly^{23} and Tyr^{24}) correlate with solvent accessibility (24), Gly^{23} and Tyr^{24} most likely initiate the first turn of the subsequent hydrophobic TM α-helix.

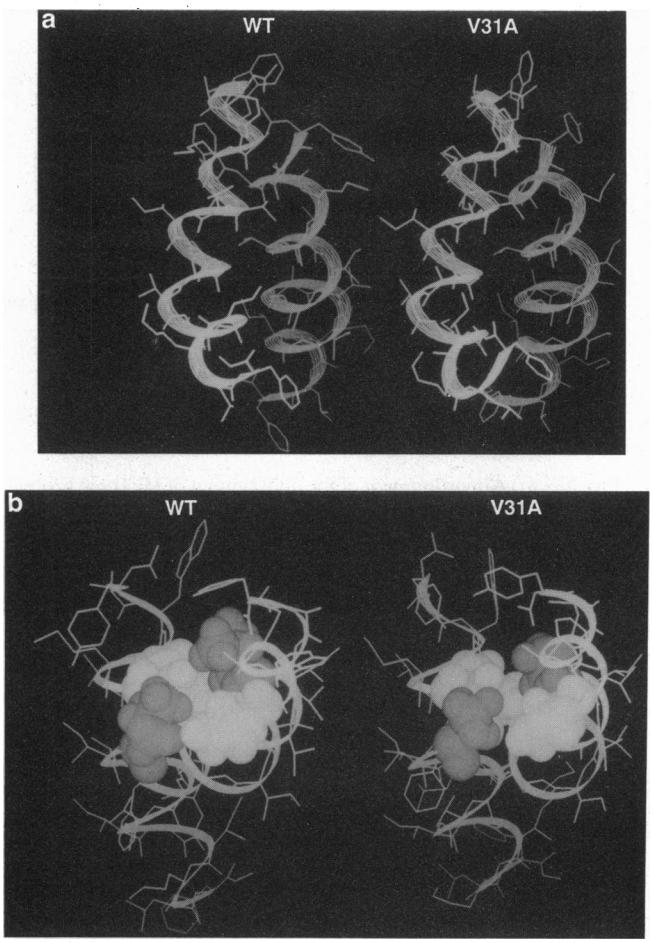

FIG. 4. Models of energy-minimized helical dimer structures of TM segments (residues 24–42 shown) of WT and mutant V31A M13 coat protein. (*a*) Helical ribbon models of energy-minimized dimers. (*b*) Detail of the mid-TM region packing face involving Val^{30} and Val^{31}. In WT (*Left*), Val^{30} (white) and Val^{31} (gray) residues of each chain are shown in space-filling representation; in mutant V31A, Val^{30} (white) and Ala^{31} (gray) are similarly indicated.

The ease with which each of the four WT M13 coat protein valine residues mutates to alanine may imply initially that wherever it occurs, Val → Ala should be considered essentially a universal replacement in membrane environments. Factors generally stabilizing a Val → Ala substitution could include the possibility of tighter protein–protein packing due to reduction in side-chain volume, as well as an inherent gain in α-helical stability in Val → Ala mutants due to reduction of strain (25). However, while mutants V29A, V30A, V31A, and V33A are chemically and hydrophobically "identical" proteins, the variation in their species formation/stability on gels and in CD spectra (Figs. 2 and 3), and the range of >18°C in their α-helix → β-sheet transition temperatures—resulting in two distinct categories of proteins [viz., (WT, V29A, V33A) vs. (V30A, V31A, V29A-V31A)]—suggests that certain WT intramembranous valine residues may be further functionalized. Consistent with these data modeling studies locate Val^{30} and Val^{31} in the protein–protein packing interface (Fig. 4).

The scope and pattern(s) of 61 viable single- and multiple-site coat protein TM-region mutants (Table 1), in conjunction with the above experimental and modeling studies, allow us to apportion the region 21–39 of WT M13 coat protein into "subdomains" and to ascribe positional roles to various TM residues (Fig. 5*a*). [Preliminary results indicate that Lys^{40}, Leu^{41}, and Phe^{42} are essentially nonmutable by the method described here (M.G. and C.M.D., unpublished work)]. That the segment 21–27 is susceptible to such a variety of polar

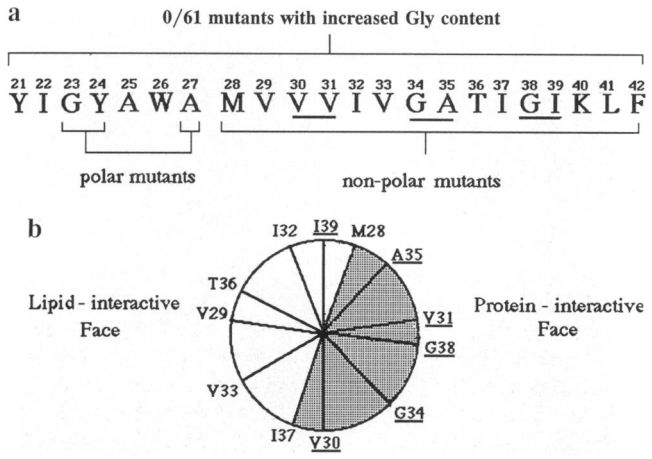

FIG. 5. (*a*) Apportionment of the midsegment of M13 coat protein (Tyr^{21}–Phe^{42}) into subdomains, as determined from mutational and structural analysis of a library of 61 viable mutant proteins. Residues underlined are those deduced to be participatory in the protein–protein packing interface within the TM hydrophobic core domain of the effective transmembrane segment. (*b*) Helical wheel representation of the TM hydrophobic core domain (Met^{28}–Ile^{39}), indicating approximate protein-interactive (shaded area) and lipid-interactive faces which arise from a four-residue (two in, two out) repeat motif. Underlined residues are as given in *a* above.

mutations (Fig. 1) emphasizes its largely aqueous-accessible location and its effective independence from the hydrophobic core domain. This result also provides a caveat that an uninterrupted stretch of uncharged residues in a protein (e.g., Tyr^{21}–Ile^{39}) may not necessarily represent the demarcation points of membrane entry/exit. The hydrophobic core of the WT TM helix (Met^{28}–Ile^{39}) may be qualitatively partitioned further into protein-interactive residues (Val^{30}-Val^{31}, Gly^{34}-Ala^{35}, Gly^{38}-Ile^{39}) and membrane-interactive residues (Met^{28}-Val^{29}, Ile^{32}-Val^{33}, Thr^{36}-Ile^{37}). This situation is depicted for the TM hydrophobic core Met^{28}–Ile^{39} in the schematic helical wheel representation shown in Fig. 5*b*. Near the extremes of the TM segment, the amphipathic character of the Trp^{26} indole side chain may aid in positioning the protein chain at the outer membrane/water interface, while the Lys^{40} side chain, although charged, may extend toward the opposing membrane/water interface from within the membrane via its side chain of four methylene groups.

Among "small" residues in the WT M13 coat protein TM segment, Gly^{34} and Ala^{35} were nonmutable (Table 1), whereas Gly^{38} tolerated only a (small) serine side chain; these three residues, in concert with Ala^{27} (all located on the same face of an α-helix in the helical wheel schematic) could facilitate the close approach of protein chains in dimerization or oligomerization. Stable dimers such as the single-spanning protein glycophorin A similarly have subunit interactions between TM segments stabilized by the close approach of faces rich in glycine and alanine residues (26). Yet the mix of "small" and "large" side chains lining the M13 coat protein packing interface (underlined in Fig. 5*a*) apparently functions to modulate the tenacity of intramembranous protein–protein interactions. Since the species required *in vivo* for the transient membrane-interactive phase of the M13 phage life cycle are not yet known, it should be emphasized that those Val → Ala mutations which enhance protein dimer stability in the M13 system are not necessarily "better" for phage viability. However, the phenomenon of dimeric (and oligomeric) helical species formation by M13 coat protein may serve as a model for multiple-spanning membrane proteins, where folding to a final tertiary structure may depend upon similar specific TM side chain–side chain interactions.

Our results suggest that Val → Ala mutations have variable impacts on stabilization of helical structures which depend upon their positions in the TM sequence. Thus, an interior Val → Ala mutation one helical turn from the packing interface of a Gly-Ala locus can dramatically increase the propensity toward helix–helix association. Given the dearth of crystallographic data on membrane proteins, the present approach provides a method for distinguishing between protein-facing and lipid-facing residues in helical assemblies. Residues identified as "out" or "in" in Fig. 5 for the M13 TM segment match, in part, the situation found in the crystal structure of the bacterial photosynthetic reaction center, where TM residue contacts were similarly correlated with patterns of helical periodicity (27). Our observation of an ≈4-residue (2 in, 2 out) helix packing motif parallels the identification by Lemmon *et al.* (28) of sensitive positions occurring with a 3.9-residue repeat along the TM helix of dimeric glycophorin A. The findings reinforce the notion of the TM segment as an independent, functional domain and confirm the sequence-dependent capacity of specific residues within this domain to modulate protein–protein interactions which underlie certain regulatory events in membrane proteins.

This work was supported in part by grants to C.M.D. from the Medical Research Council of Canada (MT-5810) and the National Cancer Institute of Canada. Z.L. is the recipient of a Medical Research Council of Canada studentship.

1. Chou, P. Y. & Fasman, G. D. (1978) *Adv. Enzymol.* **47**, 45–148.
2. Deber, C. M., Brandl, C. J., Deber, R. B., Hsu, L. C. & Young, X. K. (1986) *Arch. Biochem. Biophys.* **251**, 68–76.
3. Wickner, W. (1988) *Biochemistry* **27**, 1081–1086.
4. Fuh, G., Cunningham, B. C., Fukunaga, R., Nagata, S., Goeddel, D. V. & Wells, J. A. (1992) *Science* **256**, 1677–1680.
5. Deber, C. M., Li, Z., Joensson, C., Glibowicka, M. & Xu, G.-Y. (1992) *J. Biol. Chem.* **267**, 5296–5300.
6. Henry, G. D. & Sykes, B. D. (1990) *Biochem. Cell. Biol.* **68**, 318–329.
7. Dunker, A. K., Ensign, L. D., Arnold, G. E. & Roberts, L. M. (1991) *FEBS Lett.* **292**, 271–274.
8. Spruijt, R. B. & Hemminga, M. A. (1991) *Biochemistry* **30**, 11147–11154.
9. Randall, L. L. & Hardy, S. J. S. (1989) *Science* **243**, 1156–1158.
10. Kuhn, A. & Wickner, W. (1985) *J. Biol. Chem.* **260**, 15907–15913.
11. Spruijt, R. B., Wolfs, C. J. & Hemminga, M. A. (1989) *Biochemistry* **28**, 9158–9165.
12. Henry, G. D. & Sykes, B. D. (1992) *Biochemistry* **31**, 5284–5297.
13. Shon, K.-J., Kim, Y., Colnago, L. A. & Opella, S. J. (1991) *Science* **252**, 1303–1305.
14. Li, Z., Glibowicka, M., Joensson, C. & Deber, C. M. (1993) *J. Biol. Chem.* **268**, 4584–4587.
15. Li, Z. & Deber, C. M. (1991) *Biochem. Biophys. Res. Commun.* **280**, 687–693.
16. Taylor, J. W., Ott, J. & Eckstein, F. (1985) *Nucleic Acids Res.* **13**, 8765–8785.
17. Hubner, P., Iida, S. & Arber, W. (1988) *Gene (Amst.)* **73**, 319–325.
18. Henry, G. D., Weiner, J. H. & Sykes, B. D. (1986) *Biochemistry* **25**, 590–598.
19. Brooks, B. R., Bruccoleri, R. E., Olafson, B. D., States, D. J., Swaminathan, S. & Karplus, M. (1983) *J. Comp. Chem.* **4**, 187–217.
20. Wang, J. & Pullman, A. (1991) *Biochim. Biophys. Acta* **1070**, 493–496.
21. Wang, J. & Pullman, A. (1991) *Chem. Phys. Lipids* **57**, 1–16.
22. Nakashima, Y., Frangione, B., Wiseman, R. L. & Konigsberg, W. (1981) *J. Biol. Chem.* **256**, 5792–5797.
23. Bowie, J. U., Reidhaar-Olson, J. F., Lim, W. A. & Sauer, R. T. (1990) *Science* **247**, 1306–1310.
24. Reidhaar-Olson, J. F. & Sauer, R. T. (1988) *Science* **241**, 53–57.
25. Dao-Pin, S., Baase, W. A. & Matthews, B. W. (1990) *Proteins Struct. Funct. Genet.* **7**, 198–204.
26. Lemmon, M. A., Flanagan, J. M., Hunt, J. F., Adair, B. D., Bormann, B.-J., Dempsey, C. E. & Engelman, D. M. (1992) *J. Biol. Chem.* **267**, 7683–7689.
27. Rees, D. C., Komiya, H., Yeates, T. O., Allen, J. P. & Feher, G. (1989) *Annu. Rev. Biochem.* **58**, 607–633.
28. Lemmon, M. A., Flanagan, J. M., Treutlein, H. R., Zhang, J. & Engelman, D. M. (1992) *Biochemistry* **31**, 12719–12725.